BIOLOGY OF REPRODUCTION **84,** 505–513 (2011)
Published online before print 27 October 2010.
DOI 10.1095/biolreprod.110.083865

Thrombophilic-Type Placental Pathologies and Skeletal Growth Delay Following Maternal Administration of Angiostatin$_{4.5}$ in Mice

Catrin S. Rutland,[3] Sarah D. Atkinson,[4] Mallinath Mukhopadhyay,[2,5] Keyi Jiang,[7] Gerald A. Soff,[8] Terry M. Mayhew,[6] and Christopher A. Mitchell[1,4]

School of Veterinary Medicine and Science,[3] University of Nottingham, Sutton Bonington Campus, Leicestershire, United Kingdom
Centre for Molecular Biosciences,[4] University of Ulster at Coleraine, Coleraine, United Kingdom
School of Human Development,[5] City Hospital, and School of Biomedical Sciences,[6] Queens Medical Centre, University of Nottingham, Nottingham, United Kingdom
Feinberg Medical School,[7] Northwestern University, Chicago, Illinois
Department of Hematology,[8] Memorial Sloan-Kettering Cancer Center, New York, New York

ABSTRACT

During placentation, the concentration of fibrinous deposits on the surfaces of maternal vasculature plays a role in villous development and has been strongly implicated in the pathophysiology of human fetal growth restriction (FGR). Fibrinous deposits are conspicuous sites of platelet aggregation where there is local activation of the hemostatic cascade. During activation of the hemostatic cascade, a number of pro- and antiangiogenic agents may be generated at the cell surface, and an imbalance in these factors may contribute to the placental pathology characteristic of FGR. We tested the hypothesis that angiostatin$_{4.5}$ (AS$_{4.5}$), a cleavage fragment of plasminogen liberated at the cell surface, is capable of causing FGR in mice. Increased maternal levels of AS$_{4.5}$ in vivo result in reproducible placental pathology, including an altered vascular compartment (both in decidual and labyrinthine layers) and increased apoptosis throughout the placenta. In addition, there is significant skeletal growth delay and conspicuous edema in fetuses from mothers that received AS$_{4.5}$. Maternally generated AS$_{4.5}$, therefore, can access maternal placental vasculature and have a severe effect on placental architecture and inhibit fetal development in vivo. These findings strongly support the hypothesis that maternal AS$_{4.5}$ levels can influence placental development, possibly by directly influencing trophoblast turnover in the placenta, and contribute to fetal growth delay in mice.

angiostatin, embryo, growth restriction, placenta, trophoblast

INTRODUCTION

Fetal growth restriction (FGR) is a serious cause of perinatal morbidity and mortality associated with an increased risk of pathological complications in adult life, including diabetes and coronary heart disease [1]. In women with a history of FGR, approximately 60%–70% of cases are associated with some form of maternal thrombophilia, of which hyperhomocysteinemia, factor V Leiden, and acquired activated protein C resistance are the conditions most commonly diagnosed [2]. In addition to the high incidence of thrombophilic disorders, FGR is also characterized by excessive placental perivillous fibrinoid, often filling the villous stroma [3], and reduced villous growth [4], resulting in overall placental insufficiency. During normal placental development, this fibrin/fibrinoid turnover is a continuous and tightly regulated process [5] that mediates the formation of villous trees [6]. The deposition of fibrinoid is the result of either activation of the hemostatic cascade on the syncytial trophoblast or perivillous aggregation of platelets [7, 8]. Activation of the hemostatic cascade at the cell surface is mediated by plasmalemmal tissue factor expression and stepwise activation of a cascade of proteolytic pro-enzymes, resulting in fibrin production; however, as a result of this process, several internal cryptic peptide fragment by-products may be produced, which have potent antiangiogenic properties [9].

Angiostatin is a potent antiangiogenic peptide proteolytically derived from plasminogen in both humans and mice [10–12]. Angiostatin may exist in a variety of isoforms and contain one or more of the five kringle domains of plasminogen [11]. While angiostatin peptides are potent inducers of endothelial apoptosis, the intact plasminogen peptide is not [13–16]. Angiostatin$_{4.5}$ (AS$_{4.5}$) is a naturally occurring isoform of angiostatin that contains the first four kringle domains and 85% of the fifth kringle domain of plasminogen [11]. AS$_{4.5}$ is generated on the surface of cells in a two-step reaction process [17, 18]. Plasminogen binds to surface globular beta-actin and is cleaved by urokinase to form the serine protease plasmin. Plasmin, which remains bound to actin, undergoes autoproteolysis within kringle 5, resulting in formation of AS$_{4.5}$. AS$_{4.5}$ no longer binds to actin and is released into the circulation [17, 18].

As villous turnover and morphology are regulated by fibrin deposition, there exists a potential cell-surface-mediated mechanism for trophoblast modulation and sites of excessive fibrin deposition such as the placenta.

In a murine model in which pregnant dams were treated with 1, 10, or 20 mg/kg of bodyweight AS$_{4.5}$, severe placental phenotypes were observed, including marked alterations in the fetal/maternal vascular ratios, ultrastructural changes in vascular morphology, and thinning of the trophoblast. Additionally, an increase in apoptosis was observed in murine placentae treated with 20 mg/kg AS$_{4.5}$. Taken together, these findings warrant further investigation of the hypothesis that

[1]Correspondence: FAX: 44 (0) 28 7032 4965;
e-mail: ca.mitchell@ulster.ac.uk
[2]Current address: Wansbeck Hospital, Ashington, Woodhorn Lane, Newcastle NE63 9JJ, United Kingdom.

Received: 24 March 2010.
First decision: 23 April 2010.
Accepted: 15 October 2010.

eISSN: 1529-7268 http://www.biolreprod.org
ISSN: 0006-3363

antiangiogenic agents generated as a result of fibrinogenesis play a role in fetoplacental development.

MATERIALS AND METHODS

Animal Model

All animal experimentation carried out in this study was approved by the local institutional (University of Nottingham, UK) animal ethics committee and conducted according to national regulations (under an approved UK Home Office Project and Personal licence) in accordance with the Guide for the Care and Use of Agricultural Animals in Agricultural Research and Teaching, published by the Consortium for Developing a Guide for the Care and Use of Agricultural Animals in Agricultural Research and Teaching, first edition, 1988; and the National Research Council publication Guide for Care and Use of Laboratory Animals (copyright 1996, National Academy of Science). Timed mating was arranged between male and female C57BL/6J mice, with the presence of the vaginal plug being used to define Embryonic Day 0.5 (E0.5). Either 0, 1, 10 or 20 mg/kg human $AS_{4.5}$ [19] was injected subcutaneously into the dorsal surfaces of pregnant dams once daily from either E4.5 to E6.5, E7.5 to E9.5, or E10.5 to E17.5. On the day after the final injection, pregnant mice were killed by cervical dislocation; gravid uteri were carefully dissected free, and, after amnionectomy, fetuses were euthanized. Fetuses and placentae were fixed overnight in either 10% buffered formal saline (BFS) for histological examination or in 2.5% glutaraldehyde in cacodylate buffer for ultrastructural analysis. Following fixation in 10% BFS, fetal brains, livers, and hearts from randomly chosen E18.5 vehicle-only treated controls and $AS_{4.5}$-treated fetuses were dissected free and blotted dry, and organ weights were recorded. Representative fetuses from each group were randomly selected to assess the extent of skeletal ossification by using Alcian blue and Alizarin Red S staining methods as previously described [20]. Measurements were made of fetal bone parameters including total numbers of ribs (and those that were fully ossified), vertebrae and tail vertebrae, lengths and diameters of upper and lower bone collars, and growth plates of the humerus, radius, ulna, femur, fibia, and tibia. Direct measurements were obtained from calibrated images captured with a light microscope.

Transmission Electron Microscopy

Randomly sampled pieces of tissue from murine placentas (n = minimum of three per group) were embedded in Epon Araldite (TAAB Laboratories Equipment Ltd., Holland), and semithin sections (~0.8-μm thickness) were cut with a Reichert-Jung Ultracut-E microtome (Germany) and stained with toluidine blue prior to selectiing areas for ultrastructural analysis. Subsequently, ultrathin sections of gold interference color (~80-nm thickness) were cut and stained with uranyl acetate and lead citrate for contrast. Sections were viewed using a JEOL JEM-1010 model transmission electron microscope (Japan) at an accelerating voltage of 80 kV. Electronic images selected by systematic uniform random sampling were captured on a Kodak Megaplus model 1.6i camera.

Stereological Analysis

Systematic random sampling was adopted because it offers increased precision in making tissue proportion and blood vessel measurements [21]. It was applied to placental sections as described previously [22], using QProdit (version 3.1) image analysis software (Leica Microsystems Imaging Solutions Ltd.) with a Leitz Dialux 20EB microscope (Leitz, Germany). Images were captured on a JVC TK-C1380 color video camera.

Tissue Proportions

Overlays of test points were randomly positioned on images, and volume densities of selected components were estimated by point-counting procedures as previously described [23]. In brief, placentae were cut in half, processed, and embedded in methyl methacrylate. Serial (1.5-μm-thick) sections of each placenta were cut and collected from four equidistant points throughout each half placenta. A minimum of 10 systematically random views from each placenta were stained with toluidine blue and analyzed with the aid of a 96-point-grid layout (this resulted in an average of 896 point counts per placenta). Placental features of the E7.5 groups were assigned to one of four tissue type groups based on their location and histological phenotype: decidual tissue, decidual blood vessels, labyrinthine tissue, and spongiotrophoblast tissue. From E10.5 and E18.5 samples, proportions of labyrinthine tissue, spongiotrophoblast, maternal blood vessels (in the decidual layer), labyrinthine blood vessels, decidua, giant spongiotrophoblast cells, yolk-sac, chorion, and Reicherts membrane were determined in each placenta. Tissue proportion refers here to the relative proportion of each tissue/blood vessel type within the whole placenta.

Blood Vessel Dimensions

For analysis of blood vessel length, transections of labyrinthine fetal blood vessels and labyrinthine maternal blood spaces were counted using unbiased counting frames as previously described [23]. A total of 10 microscopic fields (from within the labyrinthine region) per placenta were systematically randomly sampled. Images were analyzed using QProdit (version 3.1) image analysis software incorporating a two-phase measurement technique (Leica Microsystems Imaging Solutions Ltd.). Each blood vessel was manually traced, for a total of 13 423 blood vessel tracings; and then five control placentae, five placentae incubated in 1mg/kg $AS_{4.5}$, six placentae incubated in 10 mg/kg $AS_{4.5}$, and seven placentae incubated in 20 mg/kg $AS_{4.5}$ were sampled. Blood vessel lengths, cross-sectional areas, diameters, and volumes were calculated using tissue proportions and placenta volume data.

TUNEL Staining

Levels of apoptosis in E18.5 murine placentas were determined using terminal deoxynucleotidyl transferase-mediated dUTP nick end-labeling (TUNEL) with an in situ cell death detection kit (Roche, Penzberg, Germany) according to the manufacturer's instructions. TUNEL staining was performed with 5-μm-thick paraffin-embedded placenta sections. Antigen retrieval was carried out with all sections by immersion in 0.1 M citrate buffer (pH 6) and microwave irradiation at 350 W for 5 min. As a positive control, a section was treated with 3000 U/ml recombinant DNase I (Sigma-Aldrich, Dorset, U.K.) to induce DNA strand breaks prior to labeling. Tissues were mounted with Mowiol mounting medium (Polysciences Inc., Eppelheim, Germany) and imaged by confocal microscopy (SP5 model; Leica, Mannheim, Germany) at a final magnification of 400×. Five fields of view were examined for each stained section, and the number of apoptotic nuclei and the total number of nuclei were recorded for each field of view, and the percentage of apoptosis was calculated.

Dual-Staining Protocol

In order to identify the cell types undergoing programmed cell death in response to $AS_{4.5}$, we performed a dual-staining protocol using 5-μm paraffin-embedded sections. Sections were first stained with TUNEL, using the protocol described above, and then they were blocked with the appropriate animal serum. Tissue was subsequently incubated with either F4/80 (diluted 1:100; Santa Cruz Biotechnology, CA), CD31 (PECAM1; diluted 1:30; Dako, Cambridgeshire, U.K.), vimentin (diluted 1:20; Sigma-Aldrich), or cytokeratin (diluted 1:100; Sigma-Aldrich). All antibodies were diluted in phosphate-buffered saline containing 1% bovine serum albumin (Sigma, Dorset, U.K.). After sections were incubated with primary antibodies, they were probed with an appropriate secondary antibody: AlexaFluor 647 (diluted 1:100; Invitrogen, Paisley, U.K.), AlexaFluor 555 (diluted 1:100; Invitrogen), or immunoglobulin G $F(ab)_2$ fluorescein isothiocyanate (diluted 1:100; Santa Cruz Biotechnology). Cell nuclei were stained with 4′,6-diamidino-2-phenylindole dihydrochloride (DAPI; Sigma, Dorset, U.K.). Tissues were mounted by using aqueous mounting medium and examined with confocal microscopy (SP5 model; Leica) at a final magnification of 200×.

Statistical Analysis

Results were subjected to two-way ANOVA to test for the presence of main effects (treatment and gestational age) and interaction effects (treatment × age). Where necessary, post hoc Fisher's least significant difference (LSD) testing was applied. Statistical significance for apoptosis levels was tested using one-way ANOVA with LSD post hoc testing, Analyses were undertaken using SPSS version 11.0 software. A p level of <0.05 was considered significant. The sample, n, varied between 3 and 57 per group, per experiment; individual result sections and tables identify each group size.

RESULTS

$AS_{4.5}$ Causes Hypertrophy of Maternal Placental Vasculature at E7.5

The dams injected with either 1 or 10 mg/kg $AS_{4.5}$ from E4.5 and euthanized at E7.5 did not differ significantly in weight or litter size from control mice (Table 1). Fractional

TABLE 1. Maternal weight gain and fetus viability for E7.5 and E10.5, control and $AS_{4.5}$ treated mice.[a]

Fetal and maternal parameters	0 mg	1 mg	10 mg
E7.5			
Number of litters	4	4	5
Maternal weight on first injection day (E4.5)	19.2 ± 0.9	19.2 ± 0.6	19.1 ± 0.9
Maternal weight at euthanasia (E7.5)	20.0 ± 0.9	19.5 ± 0.5	20.5 ± 0.7
Total number of fetuses	26	25	39
Litter size	6.5 ± 1.9	6.3 ± 2.1	7.8 ± 1.3
E10.5			
Number of litters	6	6	6
Maternal weight on first injection day (E7.5)	22.5 ± 1.3	23.1 ± 1.3	22.9 ± 1.4
Maternal weight at euthanasia (E10.5)	24.1 ± 1.7	25.1 ± 1.3	24.6 ± 1.7
Total number of fetuses	52	57	45
Litter size	8.7 ± 1.4	9.5 ± 1.2	7.5 ± 2.2

[a] Numbers indicate mean ± standard deviation where appropriate. No statistically significant differences (using ANOVA with post hoc testing) were observed between $AS_{4.5}$ and control groups for each age.

analyses of placental tissue volume proportions revealed that the proportions of decidual blood vessels were significantly increased in animals treated with 10 mg/kg $AS_{4.5}$ (14.5% ± 5.4%) compared with those treated with 1 mg/kg $AS_{4.5}$ (5.9% ± 3.9%; $p = 0.006$) and controls treated only with vehicle (6.4% ± 2.3%; $p = 0.008$). Representative photomicrographs of placentae from controls and animals treated with 10 mg/kg $AS_{4.5}$ are shown in Figure 1A and B, respectively. All other tissue types, including decidual tissue, spongiotrophoblast, and giant trophoblast, were not significantly different ($p > 0.05$; data not shown).

Effect of $AS_{4.5}$ on Placental and Embryonic Development at E10.5

Maternal weights of dams treated with 10 mg/kg $AS_{4.5}$ from E7.5 to E9.5 and euthanized on E10.5 were equivalent to those of controls (Table 1), and there were no differences in the number of viable embryos (Table 1). The proportion of decidual blood vessels in controls was also increased at E10.5 (14.8% ± 5.1% vs. 9.6% ± 3.2%; $p = 0.045$), while the proportion of labyrinthine blood vessels decreased (5.4% ± 1.7% vs. 10.4% ± 3.5%; $p = 0.002$) compared with that of $AS_{4.5}$-treated animals. Representative photomicrographs from equivalent areas of labyrinthine placentae in E10.5 control mice and animals treated with 10 mg/kg $AS_{4.5}$ are shown in Figure 1, C and D. Ultrastructural analysis of E10.5 placentas revealed detachment of fetal vascular endothelial cells (ECs) from underlying basal lamina, substantial interstitial collagen deposition in fetal tissue, and conspicuous necrotic debris (Fig. 1F) in comparison to control samples (Fig. 1E).

Effect of $AS_{4.5}$ on Maternal and Fetoplacental Development at E18.5

There were no significant differences in maternal weight gain, fetal viability, or fetal weight in mice treated with $AS_{4.5}$ (Table 2). The gross weights of placentas from 10 mg/kg $AS_{4.5}$-treated animals were greater than those of vehicle-only treated control mice ($p < 0.05$) (Table 2). The gross wet weights of fetal hearts, livers, and brains were indistinguishable from those of control mice (Table 2). In the 20 mg/kg $AS_{4.5}$-treated group, there was a nonsignificant trend toward fetuses with lower weight, smaller size, and lower heart weight (Table 2). Fetuses from dams treated with 10 mg/kg $AS_{4.5}$ were larger along all major axes, including crown-to-rump, anteroposterior diameter, and transverse diameter ($p < 0.05$, 0.01, and 0.05, respectively) (Table 2), whereas 1 mg/kg $AS_{4.5}$-treated fetuses had an increase only in the anteroposterior dimension ($p < 0.05$) (Table 2), and fetuses treated with 20 mg/kg $AS_{4.5}$ showed a statistically significant increase in crown-to-rump length in comparison to control animals ($p < 0.001$) (Table 2). As a result of the differing fetus measurements, the lengths and diameters of several bone types were measured in the control fetuses, in those treated with 1 mg/kg, and in those treated with 10 mg/kg $AS_{4.5}$ (a full list is provided in *Materials and Methods*). Increases in radial growth plate diameter, lower radial bone collar length, and lower ulnar bone collar length were observed; however, decreases in humeral growth plate length, upper fibial bone collar length, fibial growth plate length, tibial growth plate length, and lower tibial bone collar diameter were also observed (Table 3); all other bone measurements were not significantly different.

Observation of cleared, whole-mount fetuses revealed that $AS_{4.5}$-treated mice were developmentally delayed in terms of ossification of digits, vertebrae, face, ribs, and forearms and showed conspicuous signs of nuchal edema (Fig. 1, G and H).

Effect of $AS_{4.5}$ on E18.5 Placental Tissue

Analysis of fractions of tissue types revealed that at a dose of 1 mg/kg $AS_{4.5}$, labyrinthine tissue was significantly reduced in comparison to that of controls ($p < 0.05$) (Table 4). At a dose of 10 mg/kg, the proportions of labyrinthine blood vessels/spaces were increased, and the proportions of labyrinthine tissue were decreased in comparison to that of controls ($p < 0.005$ and $p < 0.0005$, respectively) (Table 4). Placental tissue fractions from dams treated with 20 mg/kg $AS_{4.5}$ were severely affected, with decreases in both labyrinthine blood vessels/spaces and chorionic tissue ($p < 0.0005$), while proportions of decidual and labyrinthine tissue were significantly increased ($p < 0.0005$) (Table 4). Stereological analysis of vascular tissue dimensions in E18.5 placentae revealed that at a dose of 1mg/kg $AS_{4.5}$, labyrinthine fetal blood vessel length was greater than that of vehicle-only treated controls (Table 4). In 10 mg/kg-treated placentae, labyrinthine fetal blood vessel length was 73% greater ($p < 0.0005$) (Table 4 and Fig. 2, A and B). However, there were no other significant differences in vascular parameters. At a dose of 20 mg/kg $AS_{4.5}$, there were a dramatic decrease in labyrinthine fetal blood vessel length and a substantial increase in labyrinthine maternal blood space length ($p < 0.0005$ and $p < 0.005$, respectively) (Table 4). Examination of ultrastructural features of E18.5 placentas treated with either vehicle-only control (Fig. 2C) or 20 mg/kg $AS_{4.5}$ revealed evidence of large platelet aggregates (Fig. 2D) and trophoblasts with tortuous cellular processes (Fig. 2E) that had incompletely invaded maternal blood vessels (Fig. 2F). There was also evidence of perturbed

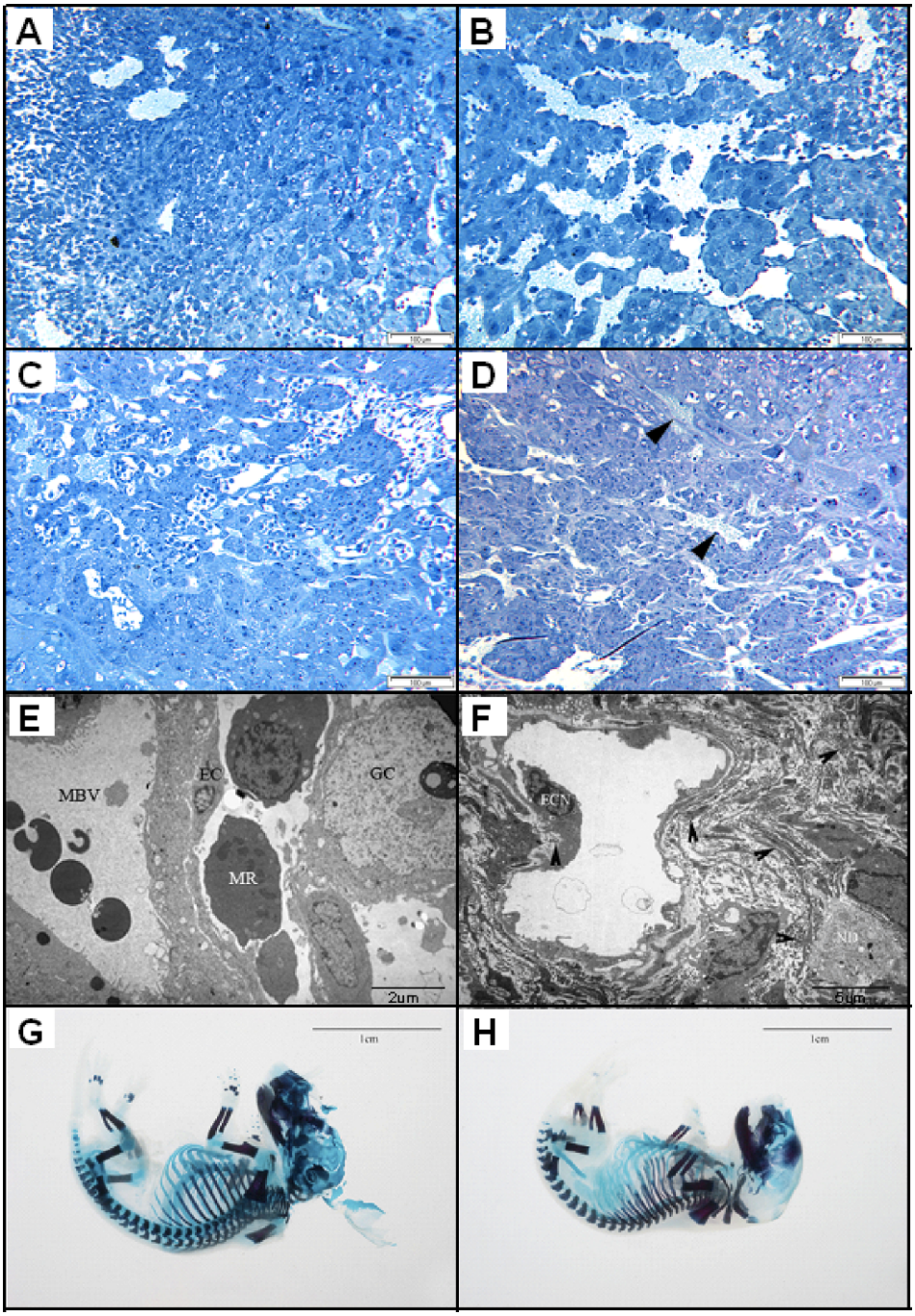

FIG. 1. Toluidine blue-stained sections are shown from E7.5 placenta of (**A**) vehicle-only treated and (**B**) 10 mg/kg $AS_{4.5}$-treated mice. Note the enlarged maternal vascular spaces in the $AS_{4.5}$-treated placenta. Toluidine blue-stained placentas from the decidual layer of an E10.5 control mouse (**C**) show numerous large-diameter blood vessels, and a 10 mg/kg $AS_{4.5}$-treated placenta (**D**) shows there are fewer and smaller caliber vessels (arrowheads). **E**) E10.5 vehicle-only treated placenta shows a maternal blood vessel (MBV) invaded by trophoblast. An endothelial cell (EC) is seen in an adjacent fetal blood vessel with fetal reticulocytes (one of which is dividing [MR]) and a nearby giant cell (GC). Note that in comparison with $AS_{4.5}$-treated dams, there is no interstitial collagen deposition. **F**) An E10.5 placenta from a dam treated with 1 mg/kg $AS_{4.5}$ shows a fetal blood vessel with an endothelial cell nucleus (ECN) partially detached from the underlying matrix and conspicuous necrotic cellular debris (ND). Collagen deposition (arrowheads) is seen immediately adjacent to the vessel and in the interstitial spaces. **G**) E18.5 fetus stained with Alizarin red and Alcian blue from a vehicle-only injected control dam and (**H**) from a 10 mg/kg $AS_{4.5}$-treated dam. In the control fetus, the ribs, metacarpals, metatarsals, and phalanges are clearly ossified. In the $AS_{4.5}$-treated pup, femoral collar lengths are shorter than in control mice, and there is poor ossification of facial bones, ribs, vertebrae, and digits, with clear evidence of nuchal edema. Bars in **A**–**D** = 100 μm; **E** = 2 μm; **F** = 5 μm; **G** and **H** = 1 cm.

cell–matrix interactions manifesting as thickening of the endothelial basal lamina with EC detachment.

$AS_{4.5}$ Increases Cellular Apoptosis in Murine Placenta

TUNEL staining was used to quantify apoptosis in E18.5 placentas treated with 20 mg/kg $AS_{4.5}$. Cell counts from positive controls (treated with DNase I prior to the addition of terminal deoxynucleotidyl transferase [TdT]), vehicle-only treated mice, and 20 mg/kg $AS_{4.5}$-treated mice were carried out, and a significant increase in apoptotic cells was observed in $AS_{4.5}$-treated placentae compared to that in control placentae ($p < 0.001$). The average number of apoptotic cells per field of view was 55 (±8.66, SEM) in the $AS_{4.5}$ group compared with 12.2 (±3.21) in the control group. Graphic representations and photomicrographs of TUNEL labeling (including positive [DNase 1-treated] control labeling) in placentae from vehicle-only treated controls and $AS_{4.5}$-injected dams are shown in Figure 3; negative control (TdT-omitted) experiments were also performed (data not shown). Primary cell types affected by administration of $AS_{4.5}$ were assessed by dual immunolabeling (Fig. 4) with TUNEL stain and antibodies to either F4/80, PECAM1 (CD31), pan-cytokeratin, or vimentin. Very few cells were shown to be colocalized with TUNEL and F4/80 or vimentin staining. The majority of colocalized signals in cell nuclei within placenta from dams treated with 20 mg/kg $AS_{4.5}$ was in the decidual and spongiotrophoblast layers (Fig. 4). Based on TUNEL staining, PECAM1 positivity, and morphology, these cells are consistent with apoptotic endothelium. Furthermore, within the spongiotrophoblast layer, a large number of cytokeratin-positive nuclei (trophoblasts) were

TABLE 2. Maternal weights and gross fetal and placental dimensions from E18.5 AS$_{4.5}$ or vehicle-only treated mice.

Weights and measurements	Treatment[a]			
Maternal weights	0 mg (7)	1 mg (3)	10 mg (4)	20 mg (4)
E10.5 (first injection day)	24.2 ± 2.1	24.9 ± 1.2	22.4 ± 2.4	25.2 ± 1.3
E18.5 (prior to euthanasia)	35.6 ± 3.1	37.6 ± 1.9	34.1 ± 3.6	38.4 ± 3.7
Placental and fetal parameters	0 mg (48)	1 mg (23)	10 mg (26)	20 mg (34)
Litter size	6.9 ± 1.6	7.7 ± 1.2	6.5 ± 1.0	8.5 ± 1.9
Placental weight (mg)	99 ± 16	103 ± 18	111 ± 14*	101 ± 19
Fetal weight (g)	1.19 ± 0.05	1.14 ± 0.08	1.23 ± 0.07	1.17 ± 0.09
Crown-rump length (mm)	21.3 ± 1.0	21.8 ± 1.1	22.1 ± 0.9*	22.3 ± 1.2***
Antero-posterior diameter (mm)	7.7 ± 0.5	8.4 ± 0.7*	8.5 ± 0.9**	8.0 ± 1.0
Transverse diameter (mm)	6.9 ± 0.6	7.3 ± 0.6	7.4 ± 0.7*	7.0 ± 0.9
Fetal organ weights	0 mg (17)	1 mg (20)	10 mg (21)	20 mg (19)
Heart (mg)	11 ± 4	11 ± 3	12 ± 2	9 ± 2
Liver (mg)	77 ± 9	77 ± 10	75 ± 12	77 ± 12
Brain (mg)	76 ± 10	74 ± 7	71 ± 9	71 ± 11

[a] Numbers in parentheses indicate number of mice analyzed. Values represent mean ± standard deviation. *P* values in comparison to control: *$P < 0.05$, **$P < 0.01$, ***$P < 0.001$.

TABLE 3. Bone measurements of E18.5 fetuses from AS$_{4.5}$ or vehicle-only treated dams.[a]

Bone measurement	Control	1 mg/kg AS$_{4.5}$[b]		10 mg/kg AS$_{4.5}$[b]	
Humeral growth plate length	2282.0 ± 96.6	2032.2 ± 169.6*	↓	2412.6 ± 78.8	-
Radial growth plate diameter	366.6 ± 33.0	332.4 ± 25.2	-	416.4 ± 40.5*	↑
Distal radial bone collar length	527.8 ± 97.3	695.8 ± 47.8***	↑	618.5 ± 47.8	-
Distal radial bone collar diameter	409.2 ± 32.0	381.0 ± 57.2	-	474.3 ± 29.2*	↑
Lower ulnar bone collar length	619.6 ± 137.3	785.0 ± 83.9*	↑	625.0 ± 34.8	-
Proximal fibular bone collar length	1056.4 ± 200.2	786.6 ± 154.2**	↓	812.0 ± 80.7*	↓
Fibular growth plate length	2113.6 ± 153.4	1782.6 ± 258.6*	↓	2100.6 ± 167.5	-
Tibial growth plate length	2230.6 ± 178.3	1880.6 ± 195.5**	↓	2273.0 ± 170.8	-
Distal tibial bone collar diameter	529.2 ± 36.0	442.0 ± 73.3*	↓	384.2 ± 58.4***	↓

[a] N = 5 per group. Values represent mean length in μm ± standard deviation. *P* values in comparison to control: *$P < 0.05$, **$P < 0.01$, ***$P < 0.005$.
[b] Arrows indicate increase or decrease in bone measurement; hyphen indicates no change.

TABLE 4. Stereological analysis of E18.5 placentas from AS$_{4.5}$ or vehicle-only treated control mice.

Analysis	Treatment[a]			
Tissue proportions	0 mg (10)	1 mg (10)	10 mg (11)	20 mg (7)
Decidual maternal blood vessels	6.3 ± 2.2	7.4 ± 2.4	7.6 ± 1.8	4.9 ± 2.1*
Giant trophoblast	0.08 ± 0.19	0.00 ± 0.00	0.00 ± 0.00	0.16 ± 0.17
Spongiotrophoblast	30.0 ± 6.3	30.6 ± 5.5	27.1 ± 3.2	30.2 ± 5.4
Reichart	3.6 ± 0.9	4.2 ± 2.8	2.9 ± 1.8	2.5 ± 1.3
Yolk sac	3.0 ± 3.8	3.9 ± 3.8	4.4 ± 3.9	1.9 ± 1.9
Labyrinthine vessels	25.9 ± 5.1	29.5 ± 6.7	34.1 ± 5.3**	23.3 ± 5.8
Decidua	3.1 ± 1.7	3.0 ± 1.5	2.0 ± 0.9	7.3 ± 1.8***
Labyrinthine tissue	14.8 ± 3.1	10.6 ± 3.5*	8.5 ± 3.6***	22.0 ± 3.8***
Chorion	13.3 ± 3.7	10.9 ± 4.9	13.3 ± 3.3	7.8 ± 1.4***
Labyrinthine vascular dimensions	0 mg (5)	1 mg (5)	10 mg (6)	20 mg (7)
Fetal blood vessel length	38.4 ± 5.5	45.9 ± 3.7*	66.5 ± 7.8***	11.2 ± 4.3***
Fetal blood vessel diameter	17.7 ± 1.1	18.2 ± 1.0	18.7 ± 1.4	16.0 ± 2.4
Maternal blood space length	30.5 ± 7.6	29.9 ± 7.2	37.9 ± 10.5	57.9 ± 20.9**
Maternal blood space diameter	20.9 ± 3.1	22.0 ± 2.9	22.7 ± 2.3	18.1 ± 2.3

[a] Numbers in parentheses indicate number of placentas analyzed. Values represent mean ± standard deviation of proportion of tissue type (% by volume), total vessel length (m), and diameter (μm). *$P < 0.05$, **$P < 0.005$, ***$P < 0.0005$.

TUNEL-positive in AS$_{4.5}$-treated placentae compared to vehicle-only treated murine placenta.

DISCUSSION

Many complications of pregnancy associated with either early fetal loss or FGR demonstrate pathophysiological hallmarks of vascular disturbance of the placenta. Pathological sequelae related to these conditions are often associated directly with poor placental perfusion or the inability to transport nutrients and dispose of waste products across the fetomaternal interface [24, 25]. Numerous studies in both human and animal models have demonstrated a clear relationship between reduction in blood flow through the placental vasculature and induction of FGR [26, 27]. Reduction in the placental vascular compartment (either fetal or maternal) or inappropriate activation of the hemostatic cascade is also linked to poor placental perfusion and FGR [28].

How reductions in fetoplacental and uteroplacental vasculature, and thus reduced placental perfusion, are linked to aberrant activation of coagulation and fibrin/fibrinoid deposition is not clear. Sites of fibrin deposition have previously been linked with increased levels of apoptosis in villi, specifically in

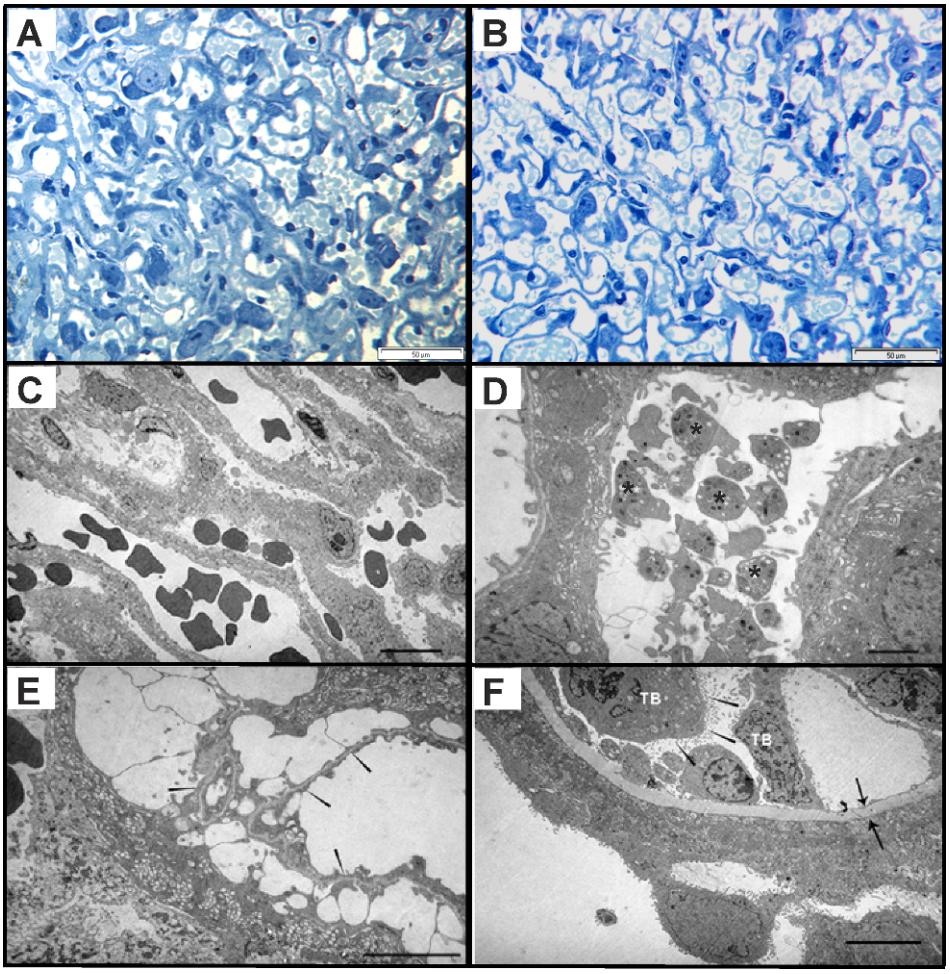

FIG. 2. Toluidine blue-stained sections from the labyrinthine tissue of placenta from (**A**) control and (**B**) 10 mg/kg $AS_{4.5}$-treated mice. Note the high proportion of fetal blood vessels (lined with endothelium) in this tissue, the relatively large nuclei of the rarified trophoblast cells, and the greatly increased fetal vasculature in comparison to that of control placentas. Ultrastructural characteristics of the labyrinthine layer from E18.5 murine placentas from dams treated with either (**C**) a vehicle-only solution or (**D–F**) 20 mg/kg $AS_{4.5}$. **D**) Large numbers of platelets (asterisks) are observed in maternal labyrinthine vessels, some of which adhere to the vessel wall. **E**) Trophoblast cells in $AS_{4.5}$-treated placentas (e.g., seen at **top right**) demonstrate tortuous extended processes wrapped around basement membrane (arrowheads) and encircling plasma-filled spaces within the vessel. **F**) Invading fetal trophoblast (TB) cells show extensive microvilli (arrowheads). Cells are incompletely attached to the wall of this maternal blood vessel, and there is an extremely thickened basement membrane (between the arrows). These features are suggestive of compromised cell–matrix interactions. Bars in **A** and **B** = 50 μm; **C–F** = 5 μm.

the trophoblast layer, which directly contacts the maternal circulation [29]. In the present study, we observed colocalization of TUNEL staining with either PECAM1- or pan-cytokeratin-labeled cells in $AS_{4.5}$-treated murine dams, consistent with endothelial/trophoblast-induced apoptosis in the maternal decidua and adjacent spongiotrophoblast tissue. Several studies have investigated the role of circulating maternal factors as possible mediators of increased levels of apoptosis in villous tissues, including vascular endothelial growth factor (VEGF), tumor necrosis factor α (TNFα) [30], and interferon-γ [31, 32], in addition to interleukins 1, 6, and 10 [33, 34]. Evidence from the current study supports the hypothesis that angiostatin, a proteolytic cleavage product of plasminogen, induces a form of FGR in mice, which is characterized by significant skeletal growth delay and edema.

In all treatment regimens used in this study, administration of $AS_{4.5}$ did not result in a reduction of maternal weight, and this is consistent with its observed lack of effect on normal tissue types in tumor-bearing models [35]. Dosing with $AS_{4.5}$ also had no effect on the number of fetuses or their weight. There are very few studies of the effects of angiogenic inhibitors during pregnancy. However, administration of TNP-470 prior to E14 has been shown to induce spontaneous abortion [36], whereas (similar to the present study's findings) treatment from E10.5–E18.5 resulted in a reproducible model of FGR with no reduction in fetal numbers [20].

Gross placental weights were not significantly different from those of vehicle-only treated placentas, except for placentae treated with 10 mg/kg $AS_{4.5}$, which were heavier ($p < 0.05$) and concomitantly showed an almost 2-fold increase in total length of labyrinthine fetal blood vessels. Placental insufficiency resulting from altered vascular dimensions leads to decreased nutrient transfer to the fetus and a decrease in overall body weight in both sheep and humans [4, 37, 38]. Although in mouse models [20] and human ''asymmetric FGR,'' the brain is invariably spared from insult, organs including the liver, kidney, heart, and thymus are usually reduced in size [27, 39, 40]. This was not the case in the present study, in which fetal organ weights in $AS_{4.5}$-treated dams were similar to those of vehicle-only treated controls. Taken together, findings of these studies are consistent with the hypothesis that the murine fetoplacental unit is able to respond rapidly to agents that target the vascular compartment by altering the fetal-to-maternal vessel ratio. Although organ weights were not greatly affected, fetal skeletal growth retardation and edema were consistently observed following administration of $AS_{4.5}$ to pregnant dams. Delayed skeletal development has been reported in fetuses from murine dams injected with lipopolysaccharide [41] and is a hallmark of human FGR [42]. Similarly, nuchal edema is associated with human FGR and other severe fetal complications [43, 44]. In the only other study in which angiostatin was administered prior to adulthood, Drixler et al. [45] administered twice-daily oral doses of angiostatin, 50 mg/kg, to mice and showed no differences in tail length, body size, or organ weights in comparison to vehicle-only treated controls. However, in that study, the angiostatin was generated from plasminogen by pancreatic elastase digestion, and the resultant angiostatin had

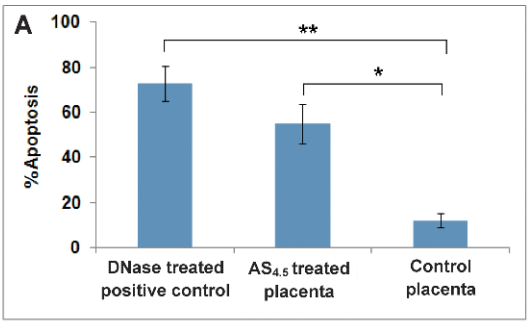

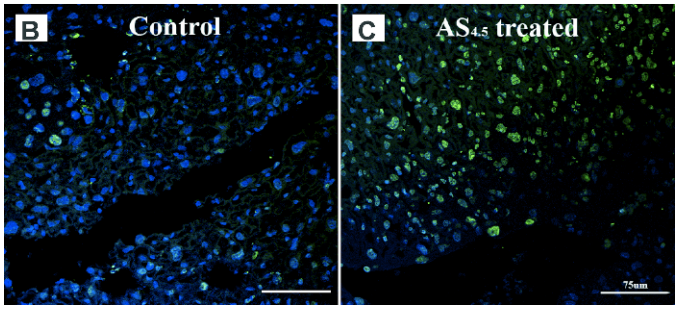

FIG. 3. Apoptotic cell counts from the positive control (treated with DNase I prior to the addition of TdT), the vehicle-only injected, and the 20 mg/kg AS$_{4.5}$-injected animals are plotted with appropriate statistical indications (**A**). Values shown are mean percentages ± standard errors of the mean of duplicate slides in five fields of view at an original magnification of ×200. Photomicrographs of apoptotic levels in E18.5 murine placentae are shown from dams treated with a vehicle-only solution (**B**) or with 20 mg/kg AS$_{4.5}$ (**C**). Statistical significance was tested using ANOVA with LSD post hoc testing, where $P < 0.001$ (*) and $P < 0.0001$ (**). Bars = 75 μm.

key structural differences from AS$_{4.5}$: in particular, it lacked the kringle 5 domain [11]. Responses to the administration of angiostatin are clearly dose- and isoform-specific, as rapid blood coagulation at the injection site accompanied by vascular activation and respiratory problems follow the administration of high doses of angiostatin (with kringle domains 1–3) in rats [46] and in intratumoral hemorrhages in humans [47].

When AS$_{4.5}$ was administered during the first half of murine pregnancy, an increase in the size of the decidual (maternal) vascular compartment of the placenta at both E7.5 and 10.5 and a concomitant decrease in the labyrinthine vasculature at E10.5 were observed. A variety of homozygous-null mutations in mice that result in embryonic lethality during mid to late gestation (including genes with a defined role in angiogenesis) demonstrate decreased size of the labyrinthine layer and an associated reduction in the fetal vascular compartment [48]. Our results indicate that an imbalance of pro- and antiangiogenic factors, termed ''angiogenic switch,'' during tumorigenesis [49] may be responsible for the deregulation of vascular growth in AS$_{4.5}$-treated placentas. Increases in the proportion of decidual maternal vasculature that we observed at E7.5 and at E10.5 are most likely a compensatory response to the EC death-inducing effects of AS$_{4.5}$ [15] via the maternal circulation.

Disturbances in placental-maternal/fetal vessel lengths have also been reported in PDGF-B/PDGF-Rβ null mice (designated *Pdgfb*^{tm1Cbet} and *Pdgfrb*^{tm1Sor}, respectively) [50], where a doubling of the fetal/maternal vessel length ratios was interpreted as a compensatory mechanism for the reduced dimensions of the maternal vasculature. In the present study, vessel lengths were affected in a dose-dependent manner, with

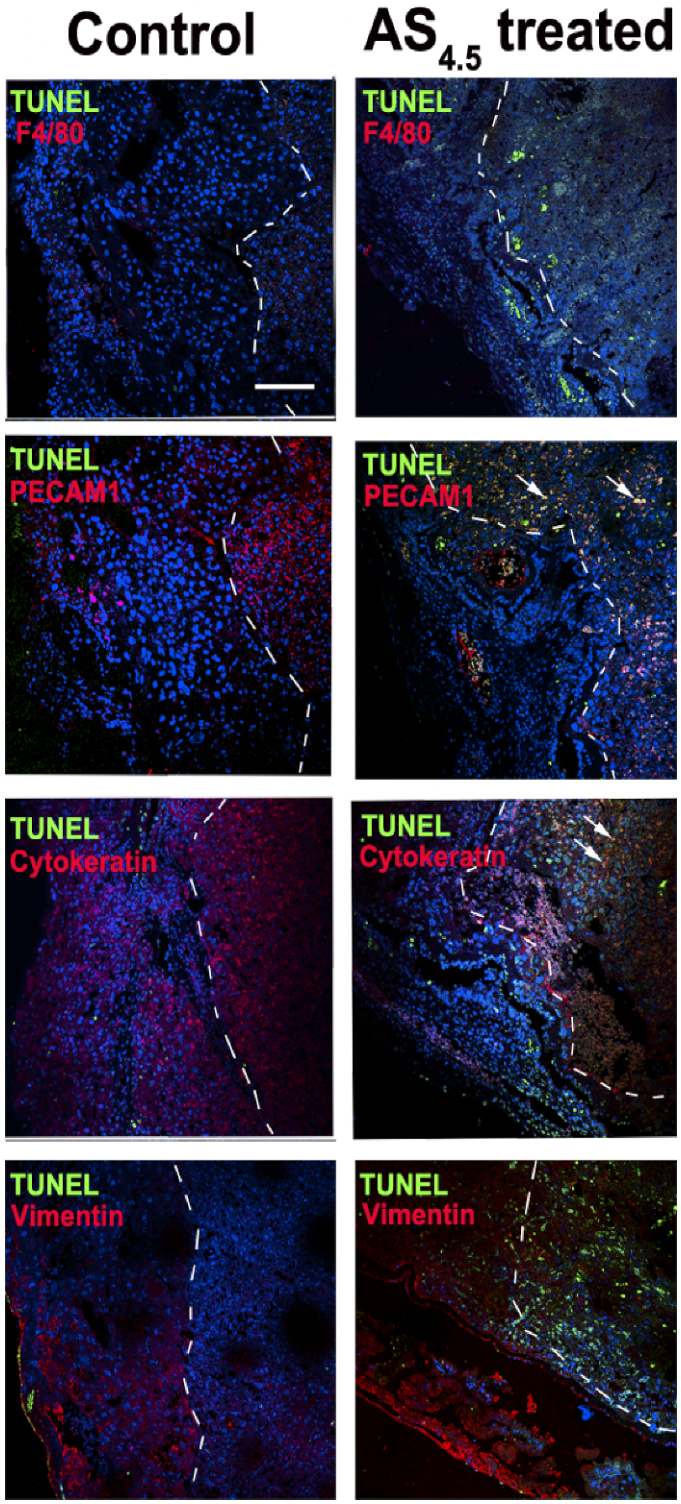

FIG. 4. Colocalization of TUNEL staining with cell markers for F4/80, cytokeratin, and vimentin in either control or AS$_{4.5}$-treated mouse placenta. Counterstaining of cell nuclei was performed with DAPI (blue). Dotted lines represent the boundary between the decidua (**left**) and the spongiotrophoblast (**right**). Significant colocalization of TUNEL with either PECAM1 or cytokeratin is represented by yellow (arrows) and is observed only in placentae from dams treated with AS$_{4.5}$. Bar = 100 μm (all panels).

both 1 and 10 mg/kg $AS_{4.5}$ leading to a ~2-fold increase in placental fetal vascular length, whereas 20 mg/kg $AS_{4.5}$ was associated with a catastrophic 71% decline in total length, which may be partially compensated by increases in total maternal labyrinthine blood space length. A higher ratio of maternal/fetoplacental vascular volumes is also implicit in morphometric data obtained from human placentas associated with FGR [51]. The effects of a single dose of angiostatin on chorioallantoic membrane vascularization in 7-day-old quail embryos revealed a decrease in vascular growth by a maximum of 68% compared to that in control embryos [52]. Similar to the 20 mg/kg $AS_{4.5}$ dose used in the current investigation, the density of blood vessels in the quail chorioallantoic membrane was markedly inhibited by the effects of angiostatin [52, 53]. Taken together, these results suggest that the effects of $AS_{4.5}$ in this model are mediated via its effects on the placenta.

Furthermore, the effects of low-dose (1 and 10 mg/kg) $AS_{4.5}$ on increasing the combined length of fetal labyrinthine blood vessels warrant further investigation. This longitudinal growth of vessels is surprising given the proapoptotic effects of angiostatin on ECs. It is possible that ECs respond to the lower doses by shape remodeling (in this case, attenuation along the vessel's long axis) in an attempt to achieve the normal developmental increase in vessel length. Such remodeling occurs in fetoplacental capillaries toward the end of human pregnancy [54]. An alternative possibility is that intercalation of circulating endothelial progenitor cells is substituted for the normal increases in vessel length, mediated by EC proliferation [55].

Similar to the findings with high doses of $AS_{4.5}$ used in this study, Battistelli et al. [3] have described some thickening of subtrophoblastic basal laminae and extracellular fibrosis within the villous stroma in cases of FGR. They attributed the stromal fibrosis to excess fibrinoid, formed in part as a coagulation product. Pierleoni et al. [56] have also shown that placental fibrinoid may be deposited not only as fibrin-type fibrinoid at the villous trophoblast surface but also as matrix-type fibrinoid in the villous stroma. Stromal accumulations of fibrinoid may be associated with alterations in cell–matrix interactions, similar to the basal lamina thickening and partial detachment of ECs observed following administration of $AS_{4.5}$ in this study. It is known that such interactions normally help to maintain vascular integrity in the maturation stage of vascular morphogenesis by stabilizing relationships among the basal lamina, extracellular matrix, ECs, and perivascular cells (notably, pericytes) [57].

In the present study, it is clear that $AS_{4.5}$ affects both maternal and fetal placental vascularization. Ultrastructural analyses of placentae revealed detachment of fetal vascular ECs from underlying basal lamina and large platelet aggregates, and trophoblasts with tortuous cellular processes had incompletely invaded maternal blood vessels. Substantial interstitial collagen deposition in fetal tissue and conspicuous necrotic debris were also detected. In addition to the placental effects, delayed ossification and nuchal edema were observed in fetuses from $AS_{4.5}$-treated dams. These findings are consistent with the hypothesis that generation of AS in areas where fibrin deposition is conspicuous (e.g., on activated endothelial cells) contributes to the pathophysiology of thrombophilic-type FGR.

ACKNOWLEDGMENTS

The authors are grateful to Dr. Trevor Grey, Department of Histopathology, Queen's Medical Centre, Nottingham, for assistance with electron microscopy, Norma Clyde for whole-mount staining, Margaret Mitchell for expertise with animal husbandry, and Suzanne Underwood for technical assistance.

REFERENCES

1. Lumbers ER, Yu ZY, and Gibson KJ. The selfish brain and the barker hypothesis. Clin Exp Pharmacol Physiol 2001; 28:942–947.
2. Kujovich JL. Thrombophilia and pregnancy complications. Am J Obstet Gynecol 2004; 191:412–424.
3. Battistelli M, Burattini S, Pomini F, Scavo M, Caruso A, Falcieri E. Ultrastructural study on human placenta from intrauterine growth retardation cases. Microsc Res Tech 2004; 65(3):150–158.
4. Mayhew TM, Ohadike C, Baker PN, Crocker IP, Mitchell C, Ong SS. Stereological investigation of placental morphology in pregnancies complicated by pre-eclampsia with and without intrauterine growth restriction. Placenta 2003; 24:219–226.
5. Mayhew TM, Barker BA. Villous trophoblast: morphometric perspectives on growth, differentiation, turnover and deposition of fibrin-type fibrinoid during gestation. Placenta 2001; 22:628–638.
6. Castellucci M, Kosanke G, Verdenelli F, Huppertz B, Kaufmann P. Villous sprouting: fundamental mechanisms of human placental development. Hum Reprod Update 2000; 6:485–494.
7. Frank HG, Malekzadeh F, Kertschanska S, Crescimanno C, Castellucci M, Lang I, Desoye G, Kaufmann P. Immunohistochemistry of two different types of placental fibrinoid. Acta Anat (Basel) 1994; 150:55–68.
8. Kaufmann P, Huppertz B, Frank HG. The fibrinoids of the human placenta: origin, composition and functional relevance. Ann Anat 1996; 178:485–501.
9. Browder T, Folkman J, Pirie-Shepherd S. The hemostatic system as a regulator of angiogenesis. J Biol Chem 2000; 275:1521–1524.
10. O'Reilly MS, Holmgren L, Shing Y, Chen C, Rosenthal RA, Moses M, Lane WS, Cao Y, Sage EH, Folkman J. Angiostatin: a novel angiogenesis inhibitor that mediates the suppression of metastases by a Lewis lung carcinoma. Cell 1994; 79:315–328.
11. Soff GA. Angiostatin and angiostatin-related proteins. Cancer Metastasis Rev 2000; 19:97–107.
12. de Groot-Besseling RR, Ruers TJ, Lamers-Elemans IL, Maass CN, de Waal RM, Westphal JR. Angiostatin generating capacity and anti-tumour effects of D-penicillamine and plasminogen activators. BMC Cancer 2006; 6:149.
13. Cao YH, Ji RW, Davidson D, Schaller J, Marti D, Sohndel S, McCance SG, O'Reilly MS, Llinas M, Folkman J. Kringle domains of human angiostatin: characterization of the anti-proliferative activity on endothelial cells. J Biol Chem 1996; 271:29461–29467.
14. O'Reilly MS, Holmgren L, Shing Y, Chen C, Rosenthal RA, Cao Y, Moses M, Lane WS, Sage EH, Folkman J. Angiostatin: a circulating endothelial cell inhibitor that suppresses angiogenesis and tumor growth. Cold Spring Harb Symp Quant Biol 1994; 59:471–482.
15. Hanford HA, Wong CA, Kassan H, Cundiff DL, Chandel N, Underwood S, Mitchell CA, Soff GA. Angiostatin(4.5)-mediated apoptosis of vascular endothelial cells. Cancer Res 2003; 63:4275–4280.
16. Lucas R, Holmgren L, Garcia I, Jimenez B, Mandriota SJ, Borlat F, Sim BK, Wu Z, Grau GE, Shing Y, Soff GA, Bouck N, et al. Multiple forms of angiostatin induce apoptosis in endothelial cells. Blood 1998; 92:4730–4741.
17. Wang H, Doll JA, Jiang K, Cundiff DL, Czarnecki JS, Wilson M, Ridge KM, Soff GA. Differential binding of plasminogen, plasmin, and angiostatin4.5 to cell surface beta-actin: implications for cancer-mediated angiogenesis. Cancer Res 2006; 66:7211–7215.
18. Wang H, Schultz R, Hong J, Cundiff DL, Jiang K, Soff GA. Cell surface-dependent generation of angiostatin4.5. Cancer Res 2004; 64:162–168.
19. Gately S, Twardowski P, Stack MS, Cundiff DL, Grella D, Castellino FJ, Enghild J, Kwaan HC, Lee F, Kramer RA, Volpert O, Bouck N, et al. The mechanism of cancer-mediated conversion of plasminogen to the angiogenesis inhibitor angiostatin. Proc Natl Acad Sci U S A 1997; 94: 10868–10872.
20. Rutland CS, Mukhopadhyay M, Underwood S, Clyde N, Mayhew TM, Mitchell CA. Induction of intrauterine growth restriction by reducing placental vascular growth with the angioinhibin TNP-470. Biol Reprod 2005; 73:1164–1173.
21. Gundersen HJ, Jensen EB. The efficiency of systematic sampling in stereology and its prediction. J Microsc 1987; 147:229–263.
22. Mayhew TM, Burton GJ. Methodological problems in placental morphometry: apologia for the use of stereology based on sound sampling practice. Placenta 1988; 9:565–581.
23. Mayhew TM. The new stereological methods for interpreting functional

morphology from slices of cells and organs. Exp Physiol 1991; 76:639–665.
24. Ehrhardt RA, Bell AW, Boisclair YR. Spatial and developmental regulation of leptin in fetal sheep. Am J Physiol Regul Integr Comp Physiol 2002; 282:R1628–R1635.
25. Pardi G, Marconi AM, Cetin I. Placental-fetal interrelationship in IUGR fetuses–a review. Placenta 2002; 23(suppl A):S136–S141.
26. Kingdom J, Huppertz B, Seaward G, Kaufmann P. Development of the placental villous tree and its consequences for fetal growth. Eur J Obstet Gynecol Reprod Biol 2000; 92:35–43.
27. Lang U, Baker RS, Braems G, Zygmunt M, Kunzel W, Clark KE. Uterine blood flow—a determinant of fetal growth. Eur J Obstet Gynecol Reprod Biol 2003; 110(suppl 1):S55–S61.
28. Younis JS, Samueloff A. Gestational vascular complications. Best Pract Res Clin Haematol 2003; 16:135–151.
29. Nelson DM. Apoptotic changes occur in syncytiotrophoblast of human placental villi where fibrin type fibrinoid is deposited at discontinuities in the villous trophoblast. Placenta 1996; 17:387–391.
30. Fukushima K, Miyamoto S, Tsukimori K, Kobayashi H, Seki H, Takeda S, Kensuke E, Ohtani K, Shibuya M, Nakano H. Tumor necrosis factor and vascular endothelial growth factor induce endothelial integrin repertories, regulating endovascular differentiation and apoptosis in a human extravillous trophoblast cell line. Biol Reprod 2005; 73:172–179.
31. Smith S, Francis R, Guilbert L, Baker PN. Growth factor rescue of cytokine mediated trophoblast apoptosis. Placenta 2002; 23:322–330.
32. Desai J, Holt-Shore V, Torry RJ, Caudle MR, Torry DS. Signal transduction and biological function of placenta growth factor in primary human trophoblast. Biol Reprod 1999; 60:887–892.
33. Greer IA, Lyall F, Perera T, Boswell F, Macara LM. Increased concentrations of cytokines interleukin-6 and interleukin-1 receptor antagonist in plasma of women with preeclampsia: a mechanism for endothelial dysfunction? Obstet Gynecol 1994; 84:937–940.
34. Neale D, Demasio K, Illuzi J, Chaiworapongsa T, Romero R, Mor G. Maternal serum of women with pre-eclampsia reduces trophoblast cell viability: evidence for an increased sensitivity to Fas-mediated apoptosis. J Matern Fetal Neonatal Med 2003; 13:39–44.
35. Lannutti BJ, Gately ST, Quevedo ME, Soff GA, Paller AS. Human angiostatin inhibits murine hemangioendothelioma tumor growth in vivo. Cancer Res 1997; 57:5277–5280.
36. Klauber N, Rohan RM, Flynn E, D'Amato RJ. Critical components of the female reproductive pathway are suppressed by the angiogenesis inhibitor AGM-1470. Nat Med 1997; 3:443–446.
37. Wallace JM, Bourke DA, Aitken RP, Leitch N, Hay WW Jr. Blood flows and nutrient uptakes in growth-restricted pregnancies induced by overnourishing adolescent sheep. Am J Physiol Regul Integr Comp Physiol 2002; 282:R1027–R1036.
38. Mayhew TM, Manwani R, Ohadike C, Wijesekara J, Baker PN. The placenta in pre-eclampsia and intrauterine growth restriction: studies on exchange surface areas, diffusion distances and villous membrane diffusive conductances. Placenta 2007; 28:233–238.
39. Gagnon R. Placental insufficiency and its consequences. Eur J Obstet Gynecol Reprod Biol 2003; 110(suppl 1):S99–S107.
40. Latini G, De Mitri B, Del Vecchio A, Chitano G, De Felice C, Zetterstrom R. Foetal growth of kidneys, liver and spleen in intrauterine growth restriction: ''programming'' causing ''metabolic syndrome'' in adult age. Acta Paediatr 2004: 93:1635–1639.
41. Xu DX, Chen YH, Zhao L, Wang H, Wei W. Reactive oxygen species are involved in lipopolysaccharide-induced intrauterine growth restriction and skeletal development retardation in mice. Am J Obstet Gynecol 2006; 195: 1707–1714.
42. Hobbins J. Morphometry of fetal growth. Acta Paediatr Suppl 1997; 423: 165–169.
43. Goldenberg A, Wolf C, Chevy F, Benachi A, Dumez Y, Munnich A, Cormier-Daire V. Antenatal manifestations of Smith-Lemli-Opitz (RSH) syndrome: a retrospective survey of 30 cases. Am J Med Genet A 2004; 124:423–426.
44. Souka AP, Krampl E, Bakalis S, Heath V, Nicolaides KH. Outcome of pregnancy in chromosomally normal fetuses with increased nuchal translucency in the first trimester. Ultrasound Obstet Gynecol 2001; 18: 9–17.
45. Drixler TA, Rinkes IH, Ritchie ED, Treffers FW, van Vroonhoven TJ, Gebbink MF, Voest EE. Angiostatin inhibits pathological but not physiological retinal angiogenesis. Invest Ophthalmol Vis Sci 2001; 42: 3325–3330.
46. Molema G, van Veen-Hof I, van Loenen-Weemaes AM, Proost JH, de Leij LF, Meijer DK. Pharmacokinetics and whole body distribution of elastase derived angiostatin (K1–3) in rats. Int J Cancer 2001; 91:1–7.
47. Beerepoot LV, Witteveen EO, Groenewegen G, Fogler WE, Sim BK, Sidor C, Zonnenberg BA, Schramel F, Gebbink MF, Voest EE. Recombinant human angiostatin by twice-daily subcutaneous injection in advanced cancer: a pharmacokinetic and long-term safety study. Clin Cancer Res 2003; 9:4025–4033.
48. Hemberger M, Cross JC. Genes governing placental development. Trends Endocrinol Metab 2001; 12:162–168.
49. Hanahan D, Folkman J. Patterns and emerging mechanisms of the angiogenic switch during tumorigenesis. Cell 1996; 86:353–364.
50. Ohlsson R, Falck P, Hellstrom M, Lindahl P, Bostrom H, Franklin G, Ahrlund-Richter L, Pollard J, Soriano P, Betsholtz C. PDGFB regulates the development of the labyrinthine layer of the mouse fetal placenta. Dev Biol 1999; 212:124–136.
51. Mayhew TM, Brotherton L, Holliday E, Orme G, Bush PG. Fibrin-type fibrinoid in placentae from pregnancies associated with maternal smoking: association with villous trophoblast and impact on intervillous porosity. Placenta 2003; 24:501–509.
52. Parsons-Wingerter P, Lwai B, Yang MC, Elliott KE, Milaninia A, Redlitz A, Clark JI, Sage EH. A novel assay of angiogenesis in the quail chorioallantoic membrane: stimulation by bFGF and inhibition by angiostatin according to fractal dimension and grid intersection. Microvasc Res 1998; 55:201–214.
53. Wang YF, Jin YF, Zhang YZ. Expression and activity determination of human angiostatin (k1–3) in culture cells and larvae of silkworm. Sheng Wu Hua Xue Yu Sheng Wu Wu Li Xue Bao (Shanghai) 2002; 34:482–487.
54. Mayhew TM, Bowles C, Yucel F. Hypobaric hypoxia and villous trophoblast: evidence that human pregnancy at high altitude (3600 m) perturbs epithelial turnover and coagulation-fibrinolysis in the intervillous space. Placenta 2002; 23:154–162.
55. Charnock-Jones DS, Kaufmann P, Mayhew TM. Aspects of human fetoplacental vasculogenesis and angiogenesis. I. Molecular regulation. Placenta 2004; 25:103–113.
56. Pierleoni C, Samuelsen GB, Graem N, Ronne E, Nielsen BS, Kaufmann P, Castellucci M. Immunohistochemical identification of the receptor for urokinase plasminogen activator associated with fibrin deposition in normal and ectopic human placenta. Placenta 1998; 19:501–508.
57. Davis GE, Senger DR. Endothelial extracellular matrix: biosynthesis, remodeling, and functions during vascular morphogenesis and neovessel stabilization. Circ Res 2005; 97:1093–1107.